6. M. Fuechsle *et al*., *Nat. Nanotechnol.* **5**, 502 (2010).
7. G. P. Lansbergen *et al*., *Nat. Phys.* **4**, 656 (2008).
8. M. Pierre *et al*., *Nat. Nanotechnol.* **5**, 133 (2010).
9. A. Morello *et al*., *Nature* **467**, 687 (2010).
10. P. M. Koenraad, M. E. Flatté, *Nat. Mater.* **10**, 91 (2011).
11. B. E. Kane, *Nature* **393**, 133 (1998).
12. R. Vrijen *et al*., *Phys. Rev. A* **62**, 012306 (2000).
13. C. D. Hill *et al*., *Phys. Rev. B* **72**, 045350 (2005).
14. L. C. L. Hollenberg, A. D. Greentree, A. G. Fowler, C. J. Wellard, *Phys. Rev. B* **74**, 045311 (2006).
15. V. Schmidt, J. V. Wittemann, S. Senz, U. Gösele, *Adv. Mater.* **21**, 2681 (2009).
16. M. T. Björk, H. Schmid, J. Knoch, H. Riel, W. Riess, *Nat. Nanotechnol.* **4**, 103 (2009).
17. A. Fuhrer, M. Füchsle, T. C. G. Reusch, B. Weber, M. Y. Simmons, *Nano Lett.* **9**, 707 (2009).
18. L. Oberbeck, N. J. Curson, T. Hallam, M. Y. Simmons, R. G. Clark, *Thin Solid Films* **464-465**, 23 (2004).
19. F. J. Ruess *et al*., *Small* **3**, 563 (2007).
20. S. R. McKibbin, W. R. Clarke, A. Fuhrer, T. C. G. Reusch, M. Y. Simmons, *Appl. Phys. Lett.* **95**, 233111 (2009).
21. G. Qian, Y.-C. Chang, J. R. Tucker, *Phys. Rev. B* **71**, 045309 (2005).
22. G. Klimeck *et al*., *IEEE Trans. Electron. Dev.* **54**, 2090 (2007).
23. S. Lee, H. Ryu, Z. Jiang, G. Klimeck, 13th International Workshop on Computational Electronics, Beijing, 27 to 29 May 2009 (2009), pp. 1–4.
24. E. Gawlinski, T. Dzurak, R. A. Tahir-Kheli, *J. Appl. Phys.* **72**, 3562 (1992).
25. F. J. Ruess *et al*., *Nanotechnology* **18**, 044023 (2007).
26. A. Yamada, Y. Jia, M. Konagai, K. Takahashi, *Jpn. J. Appl. Phys.* **28**, L2284 (1989).
27. M. Diarra, Y.-M. Niquet, C. Delerue, G. Allan, *Phys. Rev. B* **75**, 045301 (2007).
28. K. E. J. Goh, L. Oberbeck, M. Y. Simmons, A. R. Hamilton, M. J. Butcher, *Phys. Rev. B* **73**, 035401 (2006).
29. C. W. J. Beenakker, *Rev. Mod. Phys.* **69**, 731 (1997).
30. P. A. Lee, A. D. Stone, *Phys. Rev. Lett.* **55**, 1622 (1985).

Acknowledgments: This research was conducted by the Australian Research Council Centre of Excellence for Quantum Computation and Communication Technology (project number CE110001027) and the US National Security Agency and the US Army Research Office under contract number W911NF-08-1-0527. M.Y.S. acknowledges an ARC Federation Fellowship and support from the Semiconductor Research Corporation. L.H. is supported under an ARC Professorial Fellowship. National Science Foundation (NSF) supported nanoHUB.org computational resources, TeraGrid resources provided by the National Institute for Computational Sciences (NICS) and the Texas Advanced Computed Center (TACC) computational resources have been extensively used in this work. The authors declare that they have no competing financial interests.

22 September 2011; accepted 11 November 2011
10.1126/science.1214319

Candle Soot as a Template for a Transparent Robust Superamphiphobic Coating

Xu Deng,[1,2] Lena Mammen,[1] Hans-Jürgen Butt,[1] Doris Vollmer[1]*

Coating is an essential step in adjusting the surface properties of materials. Superhydrophobic coatings with contact angles greater than 150° and roll-off angles below 10° for water have been developed, based on low-energy surfaces and roughness on the nano- and micrometer scales. However, these surfaces are still wetted by organic liquids such as surfactant-based solutions, alcohols, or alkanes. Coatings that are simultaneously superhydrophobic and superoleophobic are rare. We designed an easily fabricated, transparent, and oil-rebounding superamphiphobic coating. A porous deposit of candle soot was coated with a 25-nanometer-thick silica shell. The black coating became transparent after calcination at 600°C. After silanization, the coating was superamphiphobic and remained so even after its top layer was damaged by sand impingement.

A major goal in coating research is to design self-cleaning surfaces (*1*–*4*). Many surfaces in nature are superhydrophobic; for example, lotus leaves (*5*). Mimicking their surface morphology led to the development of a number of artificial superhydrophobic surfaces (*6*, *7*), opening many applications in industrial and biological processes (*8*–*13*). Microscopic pockets of air are trapped beneath the water drops (*14*–*17*). This composite interface leads to an increase in the macroscopic contact angle and a reduced contact angle hysteresis, enabling water drops to roll off easily, taking dirt with them. However, the addition of an organic liquid such as alcohol or oil decreases the interfacial tension sufficiently to induce homogeneous wetting of the surface. Drops, initially resting on air pockets (in a Cassie state), pass the transition to complete wetting (a Wenzel state) (*14*). No naturally occurring surface is known to show a contact angle θ greater than 150° and roll-off angles below 10° for water and organic liquids. These superhydrophobic and superoleophobic surfaces are called superamphiphobic (*18*).

In contrast to superhydrophobicity, the term "superamphiphobicity" is not uniquely defined, in particular with respect to the liquid used (*19*–*22*). According to Young's equation, $\cos\Theta = (\gamma_{SV} - \gamma_{SL})/\gamma_{LV}$, the lower the surface tension, the higher the tendency of a liquid to spread on a solid surface (*22*, *23*). Here, Θ is the macroscopic contact angle, γ_{SV} is the surface tension of the solid, and γ_{SL} is the interfacial tension of the solid/liquid interface. For organic liquids ($30 \leq \gamma_{LV} \leq 18$ mN/m), mainly van der Waals interactions act between the molecules. Therefore, $\gamma_{SV} - \gamma_{SL}$ is positive, and on planar surfaces $\Theta < 90°$. Similarly, the contact angle on rough surfaces depends on the surface tensions, because roughness amplifies the wetting properties.

The key factors for superamphiphobicity are not clear yet. For water repellency, surface roughness and low surface energy are essential (*14*). To fabricate superamphiphobic surface overhangs, reentrant geometry or convex curvature is also important (*19*–*25*). The complex interplay between surface roughness, low surface energy, and topography has made it difficult and expensive to fabricate superamphiphobic surfaces. Tuteja *et al*. showed that careful design of the topography of a surface allows the construction of surfaces with a contact angle for hexadecane close to 160°, although the flat surface was oleophilic (*19*, *23*). They explained their exceptional oil-repellency by overhang structures and reentrant geometry.

Here, we describe a simple way to make robust, transparent, superamphiphobic coatings. The surface to be coated, in our case a glass slide, is held above the flame of a paraffin candle (Fig. 1A). Deposition of a soot layer turns the glass black. Scanning electron microscopy reveals that the soot consists of carbon particles with a typical diameter of 30 to 40 nm, forming a loose, fractal-like network (Fig. 1, B and C) (*26*). A water drop gently deposited on the surface shows a contact angle above 160° and rolls off easily, demonstrating the surface's superhydrophobicity (*27*). However, the structure is fragile because the particle-particle interactions are only physical and are weak. When water rolls off the surface, the drop carries soot particles with it until almost all of the soot deposit is removed and the drop undergoes a wetting transition (movie S1).

Inspired by the promising morphology of soot, we developed a technique to coat the soot layer with a silica shell, making use of chemical vapor deposition (CVD) of tetraethoxysilane (TES) catalyzed by ammonia. The soot-coated substrates were placed in a desiccator together with two open glass vessels containing TES and ammonia, respectively (fig. S1). Similar to a Stöber reaction, silica is formed by hydrolysis and condensation of TES. The shell thickness can be tuned by the duration of CVD. After 24 hours, the particles were coated by a 20 ± 5–nm–thick silica shell (Fig. 1, D and E). Calcinating the

[1]Max Planck Institute for Polymer Research, Ackermannweg 10, D-55128, Mainz, Germany. [2]Center of Smart Interfaces, Technical University Darmstadt, 64287 Darmstadt, Germany.

*To whom correspondence should be adddressed. E-mail: vollmerd@mpip-mainz.mpg.de

hybrid carbon/silica network at 600°C for 2 hours in air caused combustion of the carbon core (Fig. 1F) and a decrease in the shell thickness, but the layer kept its roughness and network texture. Only isolated chains of particles, which were not linked in the network, broke during calcination (Fig. 1B). To reduce the surface energy, the hydrophilic silica shells were coated with a semi-fluorinated silane by CVD. Therefore, the substrates and an open beaker with the volatile silane were put in a desiccator for 3 hours. After CVD, a water drop placed on top of the coating formed a static contact angle of 165° ± 1° (Fig. 2A), with a roll-off angle lower than 1°. Owing to the extremely low adhesion of the coating to water, it was difficult to deposit water drops, because they immediately rolled off (movie S2). When drops of organic liquid were deposited, the static contact angles ranged from 154° for tetradecane up to 162° for diiodomethane (Fig. 2B, Table 1, and fig. S3). The maximal roll-off angle was 5°, even for tetradecane with a surface tension of 26 mN/m.

Hexadecane drops with a radius of 1 mm, impinging with a velocity up to v = 1 m/s, did not penetrate into the layer. The drop's kinetic energy was transformed into vibrational energy, allowing the drop to rebound twice before it underwent damped oscillations and finally rested on the surface in the Cassie state (Fig. 2D, figs. S4 and S5, and table S1) (*28*–*30*). The coating retained its superamphiphobicity even after the impingement of at least thousands of water drops with a radius of 1.3 mm and a velocity of 1.4 m/s (fig. S6) or flushing of the coating with water for several hours.

At velocities between 1 and 1.5 m/s, the drop started to penetrate into the coating. As a result, a satellite drop was left on the surface after rebound. Typically at the second impact, the satellite drop merged with the primary drop and rolled off (fig. S5). Self-cleaning properties for water and alkane were verified by depositing drops of either liquid on a superamphiphobic layer and monitoring the taking up of contaminants (fig. S7).

For applications on glass surfaces such as goggles, touch screens, or difficult-to-access windows, the superamphiphobic coating needs to be thermally stable, transparent, and mechanically robust. To quantify the thermal stability, the coatings were annealed at temperatures up to 450°C for 1 hour. The static contact and roll-off angles remained constant up to 400°C (Fig. 3A). Annealing at even higher temperatures decomposed the fluorosilane. The silica network remained almost unaltered until annealed at temperatures up to 1000°C (fig. S8). Annealed coatings can recover their superamphiphobicity after repeating CVD of a fluorosilane. After calcination of the black carbon template, the silica network has a shell thickness well below the wavelength of light. Such thin shells are highly transparent, as verified by ultraviolet-visible transmittance spectra (Fig. 3B). The transmittance of a 3-μm-thick

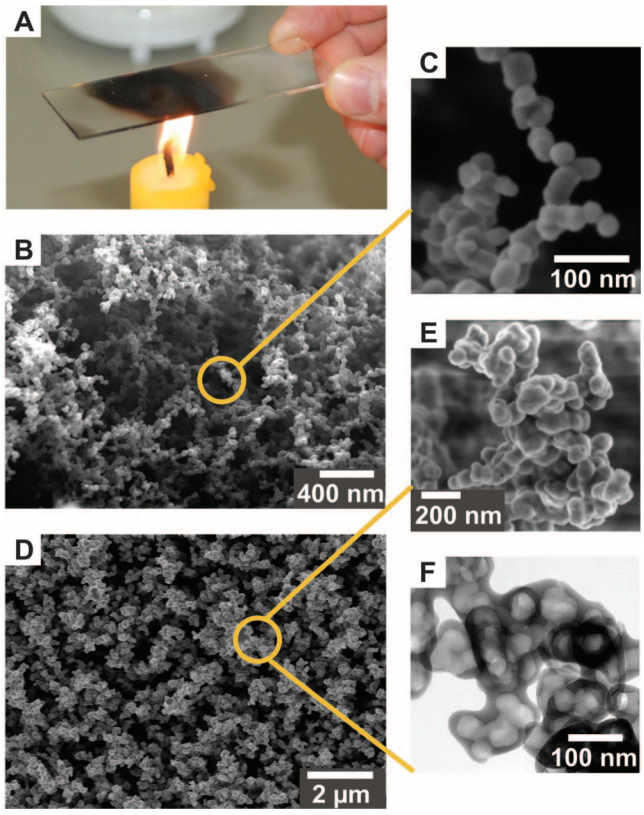

Fig. 1. Morphology of porous structure. (**A**) Photograph depicting sample preparation. A glass slide is held in the flame of a candle until a soot layer a few micrometers thick is deposited. (**B**) Scanning electron microscope (SEM) image of the soot deposit. (**C**) High-resolution SEM image showing a single particle chain made up of almost spherical carbon beads 40 ± 10 nm in diameter. (**D**) SEM image of the deposit after being coated with a silica shell (see fig. S2 for a cross section of the deposit). (**E**) High-resolution SEM image of a cluster after the carbon core was removed by heating for 2 hours at 600°C. (**F**) High-resolution TEM image of a cluster after calcination, revealing the silica coating with holes that were previously filled with carbon particles. The silica shell is 20 ± 5 nm thick.

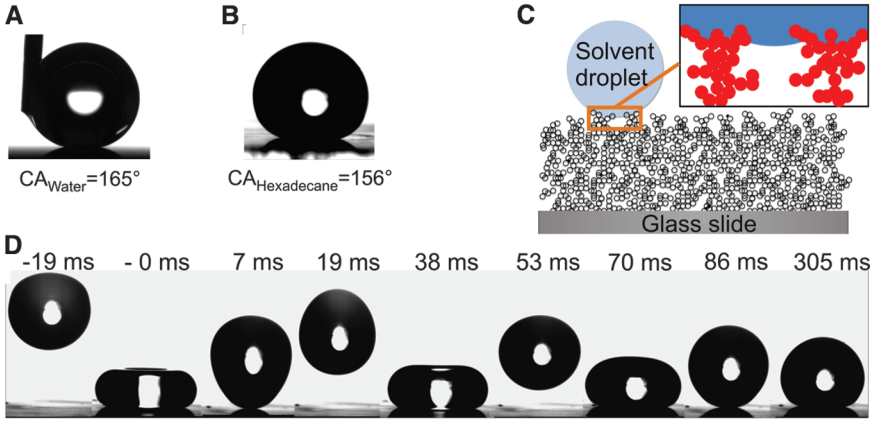

Fig. 2. Superamphiphobicity of the surface. A 2-μl water drop (**A**) and 5-μl hexadecane drop (**B**) deposited on the surface possess a static contact angle of 165° ± 1° and 156° ± 1°, respectively. (**C**) Cartoon of a liquid drop deposited on the fractal-like composite interface. (**D**) Time-resolved images of the bouncing of a 5-μl hexadecane drop on a superamphiphobic surface. Just before impinging, the drop's kinetic energy exceeds its interfacial energy by 2.4 (that is, the Weber number is 2.4) (*28*).

Table 1. Comparison of the static contact angle (SCA) and roll-off angle of drops with different surface tension, deposited on a flat fluorinated glass substrate and on a superamphiphobic coating.

Liquid	Surface tension (mN/m)	Flat surface SCA°	Superamphiphobic surface SCA°	Roll-off angle°
Water	72.1	108 ± 1	165 ± 1	1 ± 1
Diiodomethane	50.9	91 ± 1	161 ± 1	2 ± 1
Ethylene glycol	47.3	89 ± 1	160 ± 1	2 ± 1
Peanut oil	34.5	70 ± 1	158 ± 1	4 ± 1
Olive oil	32.0	69 ± 1	157 ± 1	4 ± 1
Hexadecane	27.5	64 ± 1	156 ± 1	5 ± 1
Tetradecane	26.5	54 ± 1	154 ± 1	5 ± 1

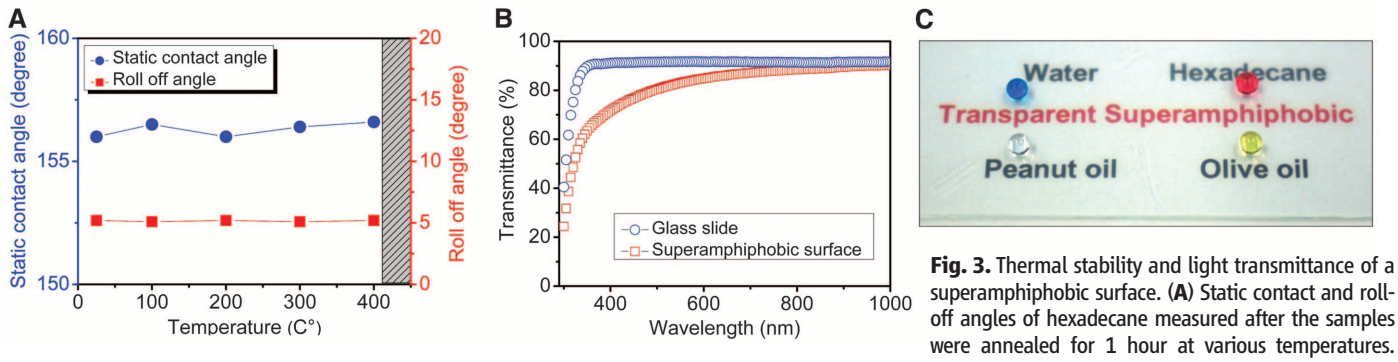

Fig. 3. Thermal stability and light transmittance of a superamphiphobic surface. (**A**) Static contact and roll-off angles of hexadecane measured after the samples were annealed for 1 hour at various temperatures. The surface loses its superamphiphobicity after annealing at temperatures above 400°C because of thermal degradation of the fluorosilane (shadow area). (**B**) Ultraviolet-visible transmittance spectra of a 3-μm-thick superamphiphobic surface compared to pristine glass. (**C**) Photograph of a drop of dyed water (γ_{lv} = 72.1 mN/m, blue); peanut oil (γ_{lv} = 34.5 mN/m, white); olive oil (γ_{lv} = 32.0 mN/m, yellow); and dyed hexadecane (γ_{lv} = 27.5 mN/m, red) deposited on a superamphiphobic glass slide. The coated slide was placed on labeled paper.

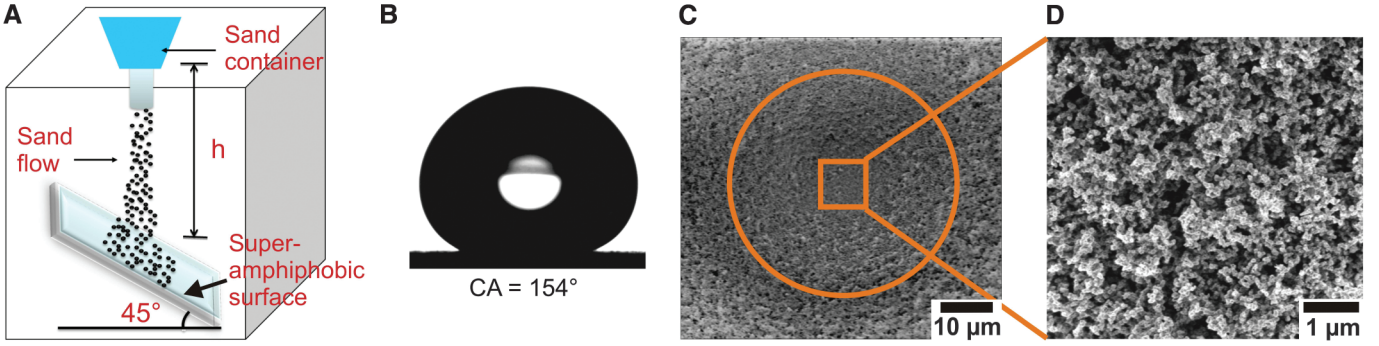

Fig. 4. Mechanical resistance quantified by sand abrasion. (**A**) Schematic drawing of a sand abrasion experiment. (**B**) Hexadecane drop deposited on the coating after 20 g of sand abrasion from 40 cm height. The 100- to 300-μm-sized grains had a velocity of 11 km/hour just before impingement. After impingement, the drops rolled off after the substrate was tilted by 5°. (**C**) SEM image of a spherical crater (orange circle) after sand abrasion. (**D**) SEM image of the surface topography inside the cavity.

coating is reduced by less than 10% as compared to that of pristine glass for wavelengths above 500 nm. This transparency is reflected in the easy readability of letters underneath the coated glass plate, and its superamphiphobicity is shown by the high contact angle for a wide variety of liquid drops (Fig. 3C).

In outdoor applications, superamphiphobic surfaces need to survive harsh conditions. To investigate the mechanical resistance of our coating, water-drop impact and sand abrasion tests were performed. Sand grains 100 to 300 μm in diameter impinged the surface from a height of 10 to ~40 cm, corresponding to an impinging energy of 1×10^{-8} to 90×10^{-8} J per grain (Fig. 4A). The silica shells were not sufficiently robust to completely resist sand impact. A cave formed underneath the impacted area (Fig. 4C). However, zooming into the cave revealed an almost unaltered submicrometer morphology (Fig. 4D). Owing to the coating's self-similarity, the surface kept its superamphiphobicity until the layer was removed after extended impact. The mechanical durability depended on the amount of sand impinging per unit of time and area, the size of the grains, the height of fall, and the thickness of the silica shell. The mechanical stability increased with the thickness of the silica shell, but at the expense of the coating's transparency. The surface retained its superamphiphobicity for 5 min of sand abrasion from a height of 25 cm (2 m/s) (movie S3). Although the coating can be eroded by wear and abrasion, it keeps its superamphiphobicity as long as its thickness remains above 2 μm (fig. S11).

The coating consists of a fractal-like assembly of nanospheres. With increasing duration of CVD of TES or annealing above 1100°C, the necks between particles fill with silica and more rod-like shapes evolve, which reduces the superamphiphobicity (figs. S8 and S10). This can be understood from Nosonovsky's prediction that convex small-scale roughness can provide a sufficient energy barrier against wetting (*22*, *31*), thus rendering superamphiphobicity possible. A spherical shape should provide a higher-energy barrier against wetting than a rod-like shape (figs. S8 and S10).

Our easy-to-fabricate oil- and water-repellent coating is made from soot encased in a silica shell. The coating is sufficiently oil-repellent to cause the rebound of impacting drops of hexadecane. Even low-surface-tension drops of tetradecane roll off easily when the surface is tilted by 5°, taking impurities along with them. The surface keeps its superamphiphobicity after being annealed at 400°C. The coating is transparent and can be applied to a variety of heat-resistant surfaces, such as aluminum, copper, or stainless steel.

References and Notes

1. H. Y. Erbil, A. L. Demirel, Y. Avci, O. Mert, *Science* **299**, 1377 (2003).
2. X. F. Gao, L. Jiang, *Nature* **432**, 36 (2004).
3. X. M. Li, D. Reinhoudt, M. Crego-Calama, *Chem. Soc. Rev.* **36**, 1350 (2007).
4. R. Blossey, *Nat. Mater.* **2**, 301 (2003).
5. W. Barthlott, C. Neinhuis, *Planta* **202**, 1 (1997).
6. L. C. Gao, T. J. McCarthy, *Langmuir* **22**, 2966 (2006).
7. X. Deng *et al.*, *Adv. Mater. (Deerfield Beach Fla.)* **23**, 2962 (2011).
8. J. Genzer, K. Efimenko, *Science* **290**, 2130 (2000).
9. S. H. Kim, S. Y. Lee, S. M. Yang, *Angew. Chem. Int. Ed.* **49**, 2535 (2010).
10. Z. Yoshimitsu, A. Nakajima, T. Watanabe, K. Hashimoto, *Langmuir* **18**, 5818 (2002).
11. G. McHale, M. I. Newton, N. J. Shirtcliffe, *Soft Matter* **6**, 714 (2010).
12. S. Shibuichi, T. Onda, N. Satoh, K. Tsujii, *J. Phys. Chem.* **100**, 19512 (1996).
13. S. Singh, J. Houston, F. van Swol, C. J. Brinker, *Nature* **442**, 526 (2006).
14. A. B. D. Cassie, S. Baxter, *Trans. Faraday Soc.* **40**, 0546 (1944).
15. A. Lafuma, D. Quéré, *Nat. Mater.* **2**, 457 (2003).

16. G. Manukyan, J. M. Oh, D. van den Ende, R. G. H. Lammertink, F. Mugele, *Phys. Rev. Lett.* **106**, 014501 (2011).
17. S. Herminghaus, *Europhys. Lett.* **52**, 165 (2000).
18. Q. Xie *et al.*, *Adv. Mater. (Deerfield Beach Fla.)* **16**, 302 (2004).
19. A. Tuteja, W. J. Choi, G. H. McKinley, R. E. Cohen, M. F. Rubner, *MRS Bull.* **33**, 752 (2008).
20. A. Steele, I. Bayer, E. Loth, *Nano Lett.* **9**, 501 (2009).
21. R. T. R. Kumar, K. B. Mogensen, P. Boggild, *J. Phys. Chem. C* **114**, 2936 (2010).
22. L. Joly, T. Biben, *Soft Matter* **5**, 2549 (2009).
23. A. Tuteja *et al.*, *Science* **318**, 1618 (2007).
24. A. Ahuja *et al.*, *Langmuir* **24**, 9 (2008).
25. L. Cao, T. P. Price, M. Weiss, D. Gao, *Langmuir* **24**, 1640 (2008).
26. C. M. Megaridis, R. A. Dobbins, *Combust. Sci. Technol* **71**, 95 (1990).
27. M. Callies, D. Quere, *Soft Matter* **1**, 55 (2005).
28. D. Bartolo *et al.*, *Europhys. Lett.* **74**, 299 (2006).
29. A. Tuteja, W. Choi, J. M. Mabry, G. H. McKinley, R. E. Cohen, *Proc. Natl. Acad. Sci. U.S.A.* **105**, 18200 (2008).
30. D. Richard, C. Clanet, D. Quéré, *Nature* **417**, 811 (2002).
31. M. Nosonovsky, *Langmuir* **23**, 3157 (2007).

Acknowledgments: We are grateful to G. Glaser, K. Kirchhoff, G. Schäfer, S. Pinnells, J. Ally, and P. Papadopoulos for technical support and stimulating discussions. We acknowledge financial support from Deutsche Forschungsgemeinschaft grants SPP 1273 (D.V.), SPP 1420 (H.J.B.), and SPP 1486 (L.M.).

Supporting Online Material

www.sciencemag.org/cgi/content/full/science.1207115/DC1
Materials and Methods
SOM Text
Figs. S1 to S11
Tables S1 and S2
References
Movies S1 to S3

8 April 2011; accepted 8 November 2011
Published online 1 December 2011;
10.1126/science.1207115

Capturing Ultrasmall EMT Zeolite from Template-Free Systems

Eng-Poh Ng,[1,2] Daniel Chateigner,[3] Thomas Bein,[4] Valentin Valtchev,[1] Svetlana Mintova[1]*

Small differences between the lattice energies of different zeolites suggest that kinetic factors are of major importance in controlling zeolite nucleation. Thus, it is critical to control the nucleation kinetics in order to obtain a desired microporous material. Here, we demonstrate how careful investigation of the very early stages of zeolite crystallization in colloidal systems can provide access to important nanoscale zeolite phases while avoiding the use of expensive organic templates. We report the effective synthesis of ultrasmall (6- to 15-nanometer) crystals of the large-pore zeolite EMT from template-free colloidal precursors at low temperature (30°C) and very high yield.

Zeolites are metastable crystalline aluminosilicate molecular sieves with uniform pores of molecular dimensions that are widely applied in catalysis, separations, and adsorption (*1*–*4*). The EMT-type zeolite has one of the lowest framework densities for a microporous material (*5*) and is a hexagonal polytype of the cubic FAU-type zeolite that plays a very important role in catalysis, for example, in fluid catalytic cracking (FCC) of hydrocarbons (*6*). Similar to the FAU-type material, the EMT framework topology has a three-dimensional large (12-membered ring) pore system. The cubic FAU polymorph features only one type of supercage (with a volume of 1.15 nm^3), but a different stacking of faujasite sheets creates two cages in the EMT zeolite: a hypocage (0.61 nm^3) and a hypercage (1.24 nm^3) (*7*). The EMT material shows interesting catalytic properties different from FAU as an FCC catalyst, but the very high price of the product so far precludes practical uses (*8*, *9*).

In addition, several EMT-FAU intergrown phases (CSZ-1, ECR-30, ZSM-20, ZSM-3) have also been reported (*9*–*14*). The synthesis of pure EMT-type zeolite is possible by templating with the expensive 18-crown-6 ether and using tightly controlled synthesis parameters (*7*). Many studies have been carried out to reduce the consumption of the crown ether template, for instance, by recycling after the synthesis (*15*) or using the so-called "SINTEF" tumbling approach (*16*, *17*), steam-assisted crystallization (*18*), surfactants (*19*), or other organic and inorganic auxiliary additives (*20*–*22*). Although the cost of producing EMT has been reduced, all attempts toward a synthesis of EMT-type zeolite without an organic structure-directing agent (OSDA) have been unsuccessful thus far. Moreover, the 18-crown-6 ether template stimulates the crystallization of micrometer-sized EMT crystals, and no attempts for the preparation of nanosized crystals have been reported.

Certain nanosized molecular sieves have been obtained at moderate (60° to 130°C) and low temperatures (25° to 50°C) (*23*–*26*). Low-temperature synthesis techniques for discrete zeolite nanocrystals from organic-free precursor systems are highly desired, as they would reduce cost and hazardous wastes, save energy, and possibly alter the properties of the materials (*26*, *27*). Here, we describe a template-free Na_2O–Al_2O_3–SiO_2–H_2O precursor system as a foundation for the preparation of a nanosized EMT molecular sieve, where the ratios between different compounds, nucleation temperature and times, and type of heating have been adjusted to avoid phase transformations (e.g., to FAU and SOD) and to stabilize the EMT-type crystals at a small particle size. We report the synthesis of ultrasmall hexagonal EMT nanocrystals (diameter of 6 to 15 nm) at the low temperature of 30°C without using any organic template; that is, from Na-rich precursor suspensions. Strikingly, this synthesis strategy requires no organic

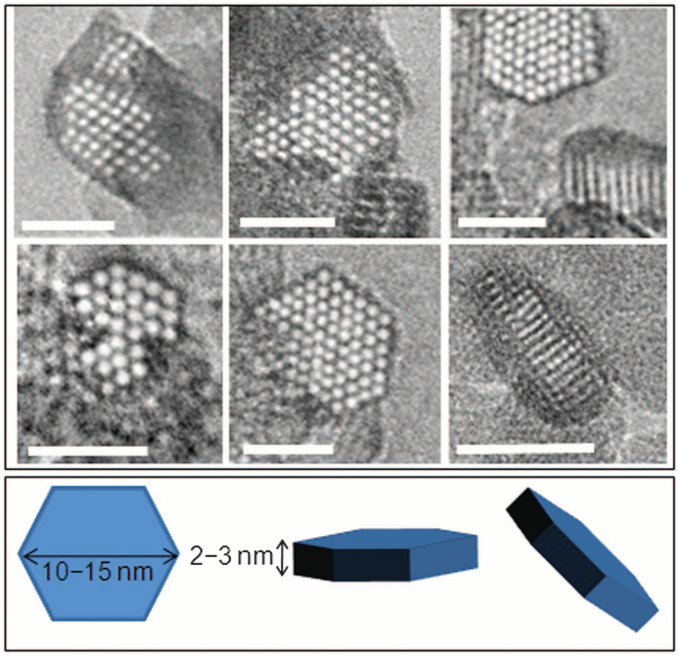

Fig. 1. Ultrasmall EMT crystals with hexagonal morphology synthesized from template-free precursor suspension at 30°C for 36 hours. The individual crystals are schematically presented with a size of 10 to 15 nm and a thickness of 2 to 3 nm. Scale bars, 10 nm.

[1]Laboratoire Catalyse and Spectrochimie, ENSICAEN, Université de Caen, CNRS, 6 Boulevard du Maréchal Juin, 14050 Caen, France. [2]School of Chemical Sciences, Universiti Sains Malaysia, 11800 USM, Pulau Pinang, Malaysia. [3]CRISMAT, ENSICAEN, Université de Caen, 6 boulevard du Maréchal Juin, 14050 Caen, France. [4]Department of Chemistry and Center for NanoScience, University of Munich (LMU), Butenandtstrasse 5-13 (E) Gerhard-Ertl-Building, 81377 Munich, Germany.

*To whom correspondence should be addressed. E-mail: svetlana.mintova@ensicaen.fr

Candle Soot as a Template for a Transparent Robust Superamphiphobic Coating

Xu Deng *et al.*

Science **335**, 67 (2012);
DOI: 10.1126/science.1207115

Science (print ISSN 0036-8075; online ISSN 1095-9203) is published weekly, except the last week in December, by the American Association for the Advancement of Science, 1200 New York Avenue NW, Washington, DC 20005.